ORIGINAL ARTICLE

A comprehensive assessment of energetic and exergetic performance for the dehumidification system of a processed pistachio production unit

Majid Dowlati Dowlati Majid Ma J. Daniel Marcos² Miguel de la Guardia⁴ l Hasan Sheikhshoaei⁵

Correspondence

Majid Dowlati, Tuyserkan Faculty of Engineering and Natural Resources, Bu-Ali Sina University, Hamedan, Iran. Email: m.dowlati@basu.ac.ir

Funding information University of Jiroft

Abstract

The present study aims to conduct a comprehensive evaluation of the energetic and exergetic performance of a dehumidification system utilized in the processing of raw pistachios. The assessment involved the application of the first and second laws of thermodynamics to calculate the exergy aspects of each component of the system, including input and output exergy rates, output/input exergy efficiency, product/fuel exergy efficiency, exergy destruction rate, exergy loss rate, exergy improvement potential rate, and specific exergy consumption. Furthermore, the effect of variations in reference state temperature on the exergy parameters was also investigated. The results indicated that the pre-dryer chamber had the highest input exergy rate among all the components of the dehumidification system. The product/fuel exergy efficiency is specified to be 35.10%, 9.47%, and 60.43%, for the electro-fan, heater, and pre-dryer chamber, respectively, while their output/input exergy efficiency are 87.87%, 22.10%, and 56.28%, respectively. The values of the exergy destruction rate of these components are 0.83, 147.14, and 1.12 kW whereas the exergy loss rate values are found to be 0.03, 4.12, and 9.24 kW, respectively. The improvement potential rate values of these components are obtained to be 0.10, 117.83, and 4.53 kW, while the amount of specific exergy consumption for the dehumidification system is determined as 481.85 kJ/kg. The study also reveals that the exergy parameters vary with changes in reference state temperature and that the exergy efficiencies decrease linearly as reference state temperature rises. Therefore, the findings of this investigation demonstrate the potential for using exergy analysis as an effective tool to improve the performance of dehumidification systems in industrial settings, specifically in the production of pistachios.

Abbreviations: EF, electro-fan; H, heater; M.C., moisture content; PC, pre-dryer chamber; w.b., wet basis.

¹Tuyserkan Faculty of Engineering and Natural Resources, Bu-Ali Sina University, Hamedan, Iran

²Department of Energy Engineering, National Distance Education University, UNED, Madrid, Spain

³Department of Process Engineering, University of Las Palmas de Gran Canaria, Las Palmas de Gran Canaria, Spain

⁴Department of Analytical Chemistry, University of Valencia, Burjassot, Spain

⁵Department of Mechanical Engineering of Biosystems, Faculty of Agriculture, University of Jiroft, Jiroft, Iran

Practical applications

Pistachio nut known as green gold because of its high economical value, is one of the popular nuts over the world. Dehumidification system based on drying technology could be used in food industry with many distinct advantages for processing of particulate crops like pistachios. For a comprehensive assessment of this system, analysis of the first and second laws of thermodynamics is applied. Exergy aspect based on the thermodynamic analysis the is an important stage for designing, modeling, optimizing, and performance assessment of the dehumidification system to produce processed pistachio. The results of this study show that the performance of dehumidification system could be improved by incorporating a steam compressor, a secondary heat exchanger, self-heat recuperation technology, and a pinch method. It is believed that such a study would contribute to the industrial exploitation of pistachio which can provide insight into decreasing energy consumption and reducing capital costs for engineers and factory owners.

KEYWORDS

dehumidification system, energy and exergy analysis, exergy destruction rate, improvement potential rate, pistachio

1 | INTRODUCTION

Pistachio (Pistacia vera L.) is a highly nutritious nut crop that holds significant economic and commercial value in several countries, including Iran, America, and Turkey. The crop is a major source of non-oil foreign exchange income, with a substantial portion of its production being exported to various regions worldwide (Mokhtarian et al., 2016). The United States, Middle Eastern, and Mediterranean countries are the primary regions where this valuable horticultural product is cultivated. Interestingly, the crop is known to be resilient to drought and salinity (Noguera-Artiaga et al., 2020). According to FAO's (2021) report, the global production of pistachio nuts was estimated at 915717.92 tons, with Iran being one of the world's largest producers and exporters, contributing around 14.74% to the total production. Based on the US Food and Drug Administration, pistachio nuts are known to contain 15 different types of micronutrients. In terms of macronutrient composition, the nuts consist of 25% protein, comprising mainly essential amino acids, 16% carbohydrates, primarily sucrose, 10% total dietary fiber, and 55% oil, with over 80% unsaturated fatty acids. Pistachio nuts are commonly available in their shells and can be sold as dried or roasted with added salt (Amiri Chayjan et al., 2017; Mandalari et al., 2021). Additionally, the kernels of the nuts find usage in various food applications, such as confectionery, pastry, ice cream, and snack foods. Pistachio butters of different types can also be produced from the kernels (Amiri Chayjan et al., 2017; Gamlı & Hayoğlu, 2007; Mandalari et al., 2021; Omid et al., 2009).

Pistachios harvested from the fields have an initial moisture content (MC) of around 40%–50% (d.b.), which is brought down to a level of 4%–6% (d.b.) through drying procedures in processing units. This is essential to preserve the nuts for long-term storage and consumption

(Kader et al., 1982; Kouchakzadeh & Haghighi, 2011). As the agricultural and horticultural industry advances, the processing of pistachios from harvest to packaging and storage is becoming increasingly mechanized. This includes the installation of processing units and industrial devices at collection terminals located in regions that are abundant in pistachios. Regardless, numerous steps are carried out in pistachio processing factories after receiving the crop, which includes (a) dehulling (b) separation of debris and empty shells (c) separation of unpeeled pistachios (d) washing (e) partial drying (f) removal of closed shells (g) thorough drying (h) separation of split nuts (i) sorting (j) salting (k) roasting (l) packaging (Kashani Nejad et al., 2003). The superior quality of pistachios in Iran, owing to favorable climatic conditions, underscores the critical role of timely processing after harvesting, particularly in the pre-drying stage, for preserving the ultimate quality of the product.

By respecting the increasing interest in shelf-stable and health-conscious items of superior quality and the evolving patterns of consumer behavior, it is incumbent upon the market to ensure the preservation of both the sensory and nutritional attributes inherent in fresh agricultural products (Beigi, 2022; Nwosu-Obieogu et al., 2022; Zalazar-Garcia et al., 2022). Generally, the drying process for pistachios requires more energy compared to other perishable fruits and vegetables due to the low thermal conductivity coefficient ranging between 0.1 and 0.2 (W/m°C) and the low heat transfer rate within the pistachio kernel, as reported in previous studies (Afzal et al., 1999; Hsu et al., 1991). Notably, about 12% of the total national industrial energy is consumed by industrial drying systems (Strumiłło et al., 1995). It is worth mentioning that industrial energy (Strumiłło et al., 1995). Therefore, the proper execution of the dehumidification or

pre-drying stage of pistachios, along with the selection of suitable methods that control air temperature, velocity, and relative humidity, not only saves energy consumption but also enhances the final product's appearance and color characteristics. This, in turn, reduces the conditions for the activity of mold-producing aflatoxin and minimizes contamination (Mokhtarian et al., 2016). Given the significance of energy consumption in industrial processing units, such as pistachio dehydrating units, examining the thermodynamic parameters of their components is crucial for energy audits. Prioritizing this examination can assist in optimizing different processing steps and ensuring the desired product quality. While an energy analysis based on the first law of thermodynamics only reports the quantity of energy in a process, it fails to differentiate the quality of different energy forms. Additionally, this analysis does not provide any indication of a thermodynamic process's inability to convert heat into mechanical work with 100% thermal efficiency, as noted by Dincer and Cengel (2001) and Chemmala and Dinesh (2014). Therefore, exergy assessment utilizing the first law (mass and energy balance) and second law of thermodynamics has proven to be an effective means of evaluating the efficient use of energy resources. This approach provides valuable and practical information about energy quality and system performance, thus overcoming the limitations and problems associated with an energy analysis based solely on the first law (Golpour et al., 2020; Parhizi et al., 2022; Zohrabi et al., 2020), Relevant research studies conducted by Argo and Ubaidillah (2020) and Moran et al. (2010) support this approach. Exergy assessment can provide a practical measure of how to approach an ideal system by identifying the sources, circumstances, and magnitude of inefficiency and irreversibility within a system. This assessment is critical in improving system efficiency, as noted by Chemmala and Dinesh (2014). The exergy index has been established as a practical instrument for enhancing the efficiency of energyconsuming units by enabling optimization, design, and retrofitting operations (Ghasemkhani et al., 2016). Unlike energy, exergy is not conserved due to the presence of irreversibility in real processes, resulting in the consumption or destruction rate of exergy. This measure signifies a flow's potential to change as it is not entirely stable in comparison to the surrounding environment (Dincer & Sahin, 2004). However, energy and exergy analysis has found practical applications in various industrial processes and systems. Tinoco-Caicedo et al. (2020) studied an exergy assessment for a spray drying system in a coffee factory for specifying the potential for energy. The results of this study showed that the overall energetic and energetic efficiencies of this system were 67.6% and 30.6%, respectively. The energy and exergy performance of onion drying in a multi-stage semi-industrial dryer was evaluated by Kaveh et al. (2021). The authors determined that increasing the air temperature and velocity at the dryer inlet resulted in higher energy consumption and exergy loss rate while decreasing the exergy efficiency. Karami et al. (2021) conducted a thermodynamic analysis of a solar hybrid forced convection dryer for rosemary drying, utilizing the first and second laws of thermodynamics. The study revealed that exergy efficiency ranged from 35% to 78%, while exergy losses and energy utilization ratio were reported to be within the range of 0.009-0.28 kJ/s and 0.24-0.50,

respectively, in another study, Bapat et al. (2016) assessed the sustainability and exergy of a quintuple evaporation unit used in a sugar production facility. The study revealed an average exergy efficiency of 91.88% and a notable improvement in the sustainability index from 3.45 to 4.45. Furthermore, in a recent study, Shen et al. (2021) executed an exergy analysis of a separation process in ethylene production. They found that the heat exchanger component had the highest exergy destruction rate, with a value of 140.28 kW. Additionally, they were able to improve the optimized efficiency of exergy by 79.53%. The authors emphasized the potential of exergy analysis in reducing energy consumption in similar processes. Zeng et al. (2022) applied an energy and exergy method to evaluate the energetic and exergetic performance of a gas-type industrial drying system of black tea. They found that the exhaust air heat loss had a major synergetic role in the exergy loss of the whole dryer unit. In addition, the exergy efficiency of the initial drying period varied from 38.08% to 65.09% and 24.76% to 26.97% while the improvement potential rate of the whole system obtained from 6.93 to 12.94 kW. Khan et al. (2016) examined an assessment to improve the process efficiency of a three-stage propane precooling cycle in the LNG process by analyzing energy and exergy indices. The study found that the highest exergy efficiency ranged between 15.51% and 18.76%. It was concluded that reducing the cooling duty in the middle stages of the propane operator could result in energy savings of up to 13.5% compared to the base case. Several scholars conducted assessments on the energy and exergy efficiencies within diverse agricultural productions such as onion (Kaveh et al., 2021), green peas (Kaveh et al., 2020), potato (Golpour et al., 2020), wheat (Yan et al., 2023), cantaloupe (Zadhossein et al., 2023), water yam (Okunola et al., 2023) and vermicelli (Kumar et al., 2023). Vilarinho et al. (2017) carried out an evaluation on the pre-distillation unit by analyzing its energy and exergy. They found that the energy and exergy efficiency of this unit were 13.40% and 2.30%, respectively. Additionally, their study identified that the thermal furnace was responsible for 15.60% of the total energy loss and 56.30% of the total exergy destruction rate in the unit. Dowlati et al. (2017) performed a detailed exergy analysis of an ice cream manufacturing plant and found that the process had an overall exergy efficiency of 2.51% and a specific exergy destruction of 791.80 kJ/kg. Various studies have explored the impact of reference state temperature on exergy efficiency in drying processes for different products using various types of dryers (Colak et al., 2013; Coskun et al., 2009; Özahi & Demir, 2013).

While various studies have investigated the exergy analysis of industrial dryers used to dry agricultural products, there is limited information available regarding the comprehensive energy and exergy evaluation of the dehumidifier unit in pistachio processing lines from an operational perspective. Therefore, the aim of this study is to gather relevant information and perform thermodynamic analysis for a comprehensive evaluation of energy and exergy. This includes obtaining thermodynamic parameters such as exergy rate and input and output exergies for each component, output/input exergy efficiency, product/fuel exergy efficiency, exergy losses,

exergy destruction rate, and exergetic improvement potential rate of all components as well as the specific exergy consumption for the relevant system. Additionally, the effect of reference state temperature on the exergy performance of the process is also investigated.

2 | MATERIALS AND METHODS

2.1 | Preparation of raw samples

The Ohadi variety of raw pistachios utilized in this research is sourced from the Kerman region, specifically harvested between late August and the end of October. Eventually, the pistachios are transported to the processing facilities of Momtazan Industries company located in Kerman.

To assess and evaluate the dehumidifier unit of the pistachio processing system, measurements were conducted during the month of August to gather the required data using the designated recording terminal. In order to determine the MC of the pistachios, samples were randomly collected from the inlet and outlet of each section and placed in sacs for storage. Subsequently, the initial MC of the pistachio samples was determined following the ASAE (2005) standard method, which involves drying the samples in an oven at 103°C for a duration of 6 h.

2.2 | Pre-drying and moistening operations

The HL 3000MD processing line, manufactured by Momtazan Industries Company in Kerman, has dimensions of 2539 cm in length, 317 cm in width, and 367 cm in height. It has a capacity of processing 3000 kg/h. The pistachio processing steps typically include peeling, separation, washing, dehumidification, dehulling, roasting, and final drying. In this study, we specifically evaluated the dehumidification unit of the processing line.

The dehumidification process is carried out prior to the roasting and final drying steps using a dedicated pistachio dehumidifier. This unit effectively removes water resulting from the washing process. By blowing hot air inside the pistachios as they pass through the device, most of their moisture is extracted. The required hot air is supplied by a heater with a specific heat capacity. Using this device results in a thorough crushing process for the pistachios, enhancing their texture and overall visual appeal. It is worth noting that the pistachios had an initial MC of approximately 38% (w.b.) when they entered the dehumidifier unit, which was subsequently reduced to 33% (w.b.) by the end of this phase. The total drying time in the final drying equipment for pistachios was determined to be 9000 s.

The dehumidifier system, illustrated in Figure 1, comprises two primary components: the heater and the pre-drying chamber. The heater, responsible for generating hot air, consists of a burner, electro-fan, and furnace, positioned adjacent to the dehumidifier. Heat is transferred from the burner to the furnace, and the resulting hot air is propelled through the furnace by the fan. The thermostat allows for temperature adjustment of the exhaust air. The heater has dimensions of 3938 mm in length, 1050 mm in width, and 1394 mm in height, with a mass of 253.40 kg. The pre-drying chamber, designed to facilitate the dehumidification and transfer of pistachios, incorporates both fixed and movable mesh plates. The movable plates, situated between the fixed plates, oscillate to gently displace the pistachios, while hot air is blown through the plates to extract moisture from the pistachios. Moreover, the transmission components consist of a shaft and a motor. The shaft undergoes intermittent motion and is efficiently connected to the motor via a mechanism that converts rotational motion into horizontal motion.

Henceforth, the heat was directed vertically onto the pistachios from below as they advanced in the process. Simultaneously, the pistachios were gently flipped multiple times to prevent any damage and enhance the overall quality. This method allowed for a thin layer and increased opening of the pistachio shells, resulting in improved quality. The primary objective of this stage was to eliminate the residual moisture absorbed during the washing process, rather than



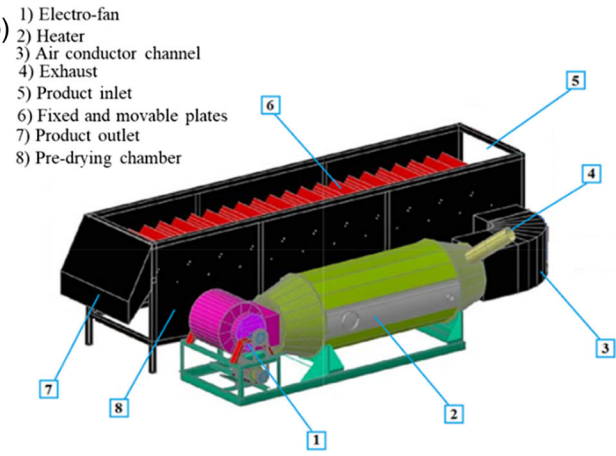


FIGURE 1 The schematic diagram of the dehumidification unit for processed pistachio production.

significantly reducing the MC of the pistachio kernels. In the final stages of pistachio processing, the kernels were subjected to a roasting period of 360 s, alongside salt. Subsequently, they were combined with a flavoring liquid and underwent a final drying process lasting 9000 s to eliminate any remaining moisture. Throughout this final drying phase, the MC of the product decreased from an initial value of 9% to 4.5% (w.b.).

2.3 | Thermodynamic evaluation of the dehumidifier system

2.3.1 | Data collection

Based on the schematic diagram of the pistachio dehumidification unit, along with the identification of the inlet and outlet flows and the knowledge of air characteristics and desired humidity, an exergy analysis was conducted for this unit considering the fuel and product parameters. The analysis involved specifying the inputs and outputs, as well as collecting data for various variables such as temperature, pressure, mass flow rate, humidity ratio, specific heat capacity, voltage, current intensity of electrical equipment, fuel consumption, electricity consumption, product moisture at inlet and outlet points, energy rate, and exergy rate. It is important to note that all the data obtained was based on the average values derived from the system's actual performance under different operating conditions. The parameters to be measured and the corresponding tools used for their measurement are provided in Table 1.

The mass flow rate of the product passing through the dehumidifier was determined by temporarily blocking the outlet and measuring the weight of the product inside a sac for a duration of 20 s. This method allowed for an accurate determination of the flow rate. To evaluate the performance of the electric motors in the system, both mechanical and electrical efficiencies were assessed using the technical specifications provided for these motors. These specifications provided the necessary data to calculate the efficiencies accurately. The thermodynamic properties of the fluids within the system were acquired by consulting thermodynamic Tables. These tables contain detailed information regarding temperature, pressure, and enthalpy, enabling the accurate analysis of the system's thermodynamic properties. Direct measurements were conducted to determine the fuel consumption of the dehumidifier. Additionally, the fuel and electricity

consumption of the other equipment in the system were obtained by monitoring the gas and electricity meters, which provided reliable data on the consumed amounts. By employing these measurement techniques and calculations, the study ensured the reliability and accuracy of the collected data.

2.3.2 | Energy and exergy analysis

To analyze the dehumidifier system, the study applied mass, energy, and exergy balance equations, which are fundamental principles derived from the first and second laws of thermodynamics. These equations allowed for the determination of important parameters such as input heat, exergy loss rate, exergy destruction rate, and exergy efficiency (Ozgener & Ozgener, 2006). The application of these equations was specifically focused on analyzing the individual components within the dehumidifier system. By considering the mass, energy, and exergy flows within each component, a comprehensive evaluation of the system's performance and efficiency was achieved. These equations provided a rigorous and systematic approach to assess the thermodynamic behavior of the dehumidifier system.

Data related to the dehumidifier used in exergy analysis

The thermal data associated with the product and fluids in the dehumidifier system (Figure 2) were utilized in the calculations and are presented in Table 2. These data were obtained from direct measurements within the dehumidifier system and have been

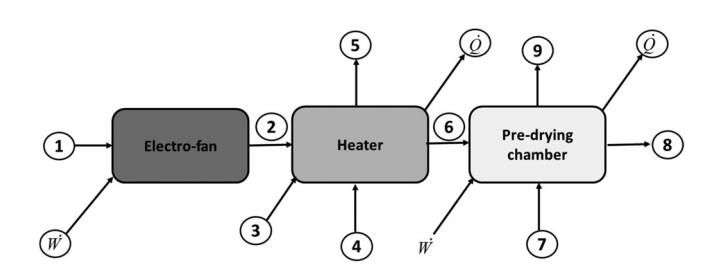


FIGURE 2 Schematic diagram of a dehumidifier system with inlet and outlet streams for each component: 1- Reference state air, 2- Air blown through the electro-fan, 3- Intake air 4- Inlet fuel (diesel), 5- Exhaust combustion gases, 6- Hot air, 7- Inlet product (wet), 8- Moist air, 9- Outlet product (dry).

TABLE 1 The details of the measurement tools and their accuracies utilized in experimental setup.

Parameters	Unit	Instrumentation	Accuracy
Reference state air temperature	C°	Sanvard SU-105 sensor	0.1 ±
Reference state air humidity	%	SAMWON ENG hygrometer	1 ±
Temperature of product	C°	Sanvard SU-105 sensor	0.1 ±
Air velocity	m/s	PROVA air flow meter with AVM-07 model	0.01 ±
Voltage of electromotor	V	A clamp ohm meter with DT266 model	1 ±
Electric current of electromotor	Α	A clamp ohm meter with DT 266 model	0.1 ±
Temperatures of air	C°	AVM-07 sensor	0.01 ±

TABLE 2 Thermal data related to the product and flows in the dehumidification system.

Value	Explanations	Parameter
273.15	Reference state temperature (K)	To
300.55- 328.57	Air temperature in different positions (K)	T _a
300.55- 308.26	Product temperature at inlet and outlet (K)	Tp
682.98	Temperature of exhaust combustion gas (K)	T_{cg}
308	Temperature of dehumidifier chamber wall (K)	T_{cw}
334.11	Heater wall temperature (K)	T_{hw}
101.1	Dead state pressure (kPa)	P_0
101.1	Inlet fuel pressure (kPa)	P_f
10.167-53	Relative air humidity (%)	Φ
33.84- 37.92	Moisture content of the product based on w.b. (%)	M_p
16	Air velocity at system inlet (m/s)	Va
4.19	Flow rate of exhaust combustion gas (m ³ /s)	v_{cg}
0.867- 0.954	Air density (kg/m³)	$ ho_a$
830	Diesel density (kg/m³)	$ ho_{f}$
0.434	Density of exhaust combustion gas (kg/m³)	$ ho_{cg}$
1.01-1.021	Specific air heat (kJ/kgK)	C_a
1.162	Specific heat of exhaust combustion gases (kJ/kgK)	C_{cg}
2.680- 2.772	Specific heat of the product (kJ/kgK)	C_p
0.287	Constant of air (kJ/kgK)	R_a
0.462	Constant of vapor (kJ/kgK)	R_{v}
0.290	Constant of exhaust combustion gases (kJ/kgK)	R_{cg}
0.003- 0.009	Vapor moisture ratio in air (kg _{water} / kg _{air})	ω
42190.00	Lower heat value of diesel (kJ/kg)	LHV

recorded using the SI system units. It is important to note that in this study, state 0 represents the reference state of the system, which is characterized by a reference temperature of 0° C and a reference pressure of 101.325 kPa.

In accordance with the schematic diagram of the dehumidifier system depicted in Figure 2, each flow within the system has been assigned a specific number. The relevant information for these flows, including temperature, pressure, mass flow rate, humidity ratio, specific heat capacity, energy rate, and exergy rate, has been documented and analyzed. These parameters provide essential insights into the thermodynamic behavior and performance of the dehumidifier system.

Assumptions

In this study, the evaluation of the exergy index was conducted under several assumptions, which are outlined as follows:

- 1. The dehumidifier unit system operated under steady-state conditions.
- 2. Fresh air and combustion gases were treated as ideal gases.
- 3. The combustion process was assumed to be a complete chemical reaction.
- 4. Kinetic and potential exergies were considered to be negligible.
- 5. The reference state temperature and pressure were assumed to be 0° C and 101.325 kPa, respectively.
- 6. Exergy analysis was performed based on the low heating value (LHV) for the fuel.
- The general equation for diesel combustion in the system was considered as follows (Hogerwaard, 2014; Kim et al., 2010):

$$C_{12}H_{23} + 17.75(O_2 + 3.76N_2) \rightarrow 12CO_2 + 11.5H_2O + 66.74N_2$$
 (1)

$$CH_4 + 2(O_2 + 3.76 N_2) \rightarrow CO_2 + 2 H_2 O + 7.52 N_2.$$
 (2)

These assumptions provide a framework for the exergy analysis conducted in the study, ensuring a consistent and reliable assessment of the system's performance.

Mass balance equations

As depicted in Figure 2, the dehumidifier system consists of various components, including the electro-fan, heater, and pre-dryer chamber. To analyze the system, mass balance equations were formulated for each component by considering the input and output flows. These equations allow for a detailed assessment of the mass flow rates within the system and contribute to a comprehensive understanding of its operation. Specifically, the electro-fan, heater, and pre-dryer chamber were subjected to individual analysis to evaluate their respective contributions to the overall performance of the dehumidifier system.

Figure 2 illustrates the presence of several mass flows within the dehumidifier system, namely air, fuel, product, product moisture, and drying air. By examining these mass flows, the mass balance equations for each component of the system can be derived as follows:

Electro-fan (EF):

$$\dot{m}_{a1} = \dot{m}_{a2}$$
 air (3)

Heater (H):

$$\dot{m}_{f4} + \dot{m}_{a3} = \dot{m}_{g5} \qquad \text{fuel} \tag{4}$$

$$\dot{m}_{a2} = \dot{m}_{a6} \quad \text{air} \tag{5}$$

Pre-dryer chamber (PC):



$$\dot{m}_{p7} = \dot{m}_{p9}$$
 product (6)

$$\dot{m}_{a6} = \dot{m}_{a8}$$
 air (7)

$$\omega_6(\dot{m}_{a6}) + (\dot{m}_{w7}) = \omega_8(\dot{m}_{a8}) + (\dot{m}_{w9})$$
 moisture (8)

Energy balance equations

Based on the comprehensive energy balance relationship, the energy rate of each flow can be determined by multiplying the mass flow rate with its specific enthalpy. Before writing the energy balance equations, it is necessary to establish the enthalpy relations associated with the mass flows in the system, as well as the relationships for heat and work calculations. The following calculations are used to determine these values:

$$\sum \dot{Q} + \sum \dot{m}_{in} h_{in} = \sum \dot{W} + \sum \dot{m}_{out} h_{out}. \tag{9}$$

The specific enthalpy of the airflow at various points in the system can be determined using Equation (10) derived from Heldman and Singh (1981):

$$h_a = c_a(T_a - T_0) + h_{fa}\omega. \tag{10}$$

The specific heat capacity of air was obtained from the following relationship (Corzo et al., 2008):

$$c_a = 1.004 + 1.88\omega. \tag{11}$$

In the energy analysis, the following relationship was used to convert relative humidity into air humidity ratio, which represents the amount of moisture in kilograms per kilogram of dry air (Akpinar, 2004):

$$\omega = 0.622 \frac{\phi P_{vs}}{P - \phi P_{vs}}. \tag{12}$$

The specific enthalpy of the product and combustion gases can be calculated using the following relations:

$$h_p = c_p (T_p - T_0) \tag{13}$$

$$h_g = c_g (T_g - T_0).$$
 (14)

The specific heat capacity of combustion gases can be calculated using the heat capacities of their individual components. The specific heat capacity of the combustion gases (c_g) can be determined using the following equation:

$$c_g = \sum X_i c_{i.} \tag{15}$$

The composition of the gases resulting from combustion and the corresponding specific heat capacity relationships are provided in Table 2.

For the electric motors in the dehumidifier system, which are of the three-phase type, the power consumption rate was determined using the equation specified by Hepbasli et al. (2010).

$$\dot{W} = \frac{\text{VI}\sqrt{3}\cos\phi}{1000}\eta_{\text{elec}}\eta_{\text{mech}}.$$
 (16)

However, for the system illustrated in Figure 2, taking into account the input and output energy terms for each component of the dehumidifier system, the energy balance equations were formulated as follows.

Electro-fan (EF):

$$\dot{En}_{a1} + \dot{W} = \dot{En}_{a2} \tag{17}$$

$$(\dot{m}_{a1})h_{a1} + \dot{W} = (\dot{m}_{a2})h_{a2}.$$
 (18)

Heater (H):

$$\dot{E}\dot{n}_{a2} + \dot{E}\dot{n}_{a3} + \dot{E}\dot{n}_{f4} = \dot{E}\dot{n}_{g5} + \dot{E}\dot{n}_{a6} + \dot{Q}_{l}$$
 (19)

$$(\dot{m}_{a2})h_{a2} + (\dot{m}_{a3})h_{a3} + (\dot{m}_{f4})LHV = (\dot{m}_{g5})h_{g5} + (\dot{m}_{a6})h_{a6} + \dot{Q}_{I}.$$
 (20)

Pre-drver chamber (PC):

$$\dot{E}\dot{n}_{a6} + \dot{E}\dot{n}_{p7} + \dot{W} = \dot{E}\dot{n}_{a8} + \dot{E}\dot{n}_{p9} + \dot{Q}_{l}$$
 (21)

$$(\dot{m}_{a6})h_{a6} + (\dot{m}_{p7})h_{p7} + \dot{W} = (\dot{m}_{a8})h_{a8} + (\dot{m}_{p9})h_{p9} + \dot{Q}_{L}$$
 (22)

Considering that diesel is utilized as the fuel for the combustion process within the heater, the LHV of diesel was considered to be 42,190 kJ/kg. The heat loss rate from the heater body (\dot{Q}_l) and the pre-dryer chamber can be determined using Equations (20) and (22), respectively.

Exergy balance equations

According to the exergy balance principle, the exergy rate of each flow within the system is determined by multiplying the mass flow rate by its specific exergy. Thus, in order to formulate the exergy balance equations, it is essential to define the specific exergy relationships for the flows in the system, which encompass energy, heat, and work transfers. Generally, neglecting nuclear and magnetic effects, the specific exergy of a flow can be expressed as (Balli et al., 2007):

$$ex = ex^{kn} + ex^{pt} + ex^{ph} + ex^{ch}$$
. (23)

The terms ex^{kn}, ex^{pt}, ex^{pt}, ex^{ph}, and ex^{ch} represent the contributions of kinetic, potential, physical, and chemical components to the total exergy, respectively. For the purpose of this study, kinetic and potential exergies are assumed to be negligible.

The specific exergy of the air flow can be determined using the following relation (Dincer & Sahin, 2004):

$$\begin{split} \text{ex}_{a} &= \left[c_{a} + \omega c_{v}\right] (T - T_{0}) - T_{0} \left\{ \left[c_{a} + \omega c_{v}\right] \ln \left(\frac{T}{T_{0}}\right) \right. \\ &- \left. \left(R_{a} + \omega R_{v}\right) \ln \left(\frac{P}{P_{0}}\right) \right\} + T_{0} \left\{ \left(R_{a} + \omega R_{v}\right) \ln \left(\frac{1 + 1.6078\omega_{0}}{1 + 1.6078\omega}\right) \right. \\ &+ 1.6078\omega R_{a} \ln \left(\frac{\omega}{\omega_{0}}\right) \right\}. \end{split}$$

The specific chemical exergy of the diesel fuel was approximated from the following relationship, which is related to the hydrocarbon fuels (C_aH_b) (Rodriguez, 1980):

$$\frac{\text{ex}_f^{\text{ch}}}{\text{LHV}} = \gamma_f = 1.04224 - 0.011925 \frac{b}{a} + \frac{0.042}{a}. \tag{25}$$

The parameter γ_f represents the fuel exergy grade function for the hydrocarbon fuel, and for diesel, it was determined to be 1.061362. The specific chemical exergy of the combustion gases can be calculated using Equation (26) as described by Soufiyan et al. (2016):

$$ex_g^{ch} = n_g \left(\sum_i y_i \delta_i + \overline{R} T_0 \sum_i y_i \ln(y_i) \right). \tag{26}$$

The composition of gases produced from diesel combustion, along with their respective mass and mole fractions and standard chemical exergy values, are provided in Table 3.

The specific physical exergy of the fuel flow, assuming constant specific heat, was calculated using the method described by Soufiyan and Aghbashlo (2017).

$$\operatorname{ex_f^{ph}} = c_f \left(T - T_0 - T_0 \ln \frac{T}{T_0} \right) - v_0 (P - P_0).$$
 (27)

The specific physical exergy of combustion gases was also obtained as follows (Kotas, 1995):

$$\operatorname{ex}_{g}^{\operatorname{ph}} = c_{g} \left(T - T_{0} - T_{0} \ln \left(\frac{T}{T_{0}} \right) \right) + RT_{0} \ln \left(\frac{P}{P_{0}} \right). \tag{28}$$

The specific exergy of the inlet fuel flow and the outlet gas flow from the heater was determined by calculating the sum of their physical and chemical exergy values, as per the comprehensive exergy balance relationship

$$ex_{f,g} = ex_{f,g}^{ch} + ex_{f,g}^{ph}.$$
 (29)

The specific physical exergy of the product flow is given as below (Beian, 1988):

$$\exp_p^{\text{ph}} = c_p \left(T - T_0 - T_0 \ln \frac{T}{T_0} \right).$$
 (30)

The specific heat capacity of the pistachio product (c_p) was determined by taking the average specific heat capacity of its components, using the following relationship as derived by Choi 1986

$$c_p = \sum c_i X_i. \tag{31}$$

The compositions of the product and their corresponding specific heat capacity relationships can be found in Table 4.

TABLE 4 Specific heat capacity (kJ/kgK) based on the temperature of the compositions of pistachio (Heldman & Singh, 1981).

Components	Formulas
Protein	$c = 2.0082 + 1.2089 \times 10^{-3} \text{T} - 1.3129 \times 10^{-6} \text{T}^2$
Fat	$c = 1.9842 + 1.4733 \times 10^{-3} \text{T} - 4.8008 \times 10^{-6} \text{T}^2$
Carbohydrate	$c = 1.5488 + 1.9625 \times 10^{-3} \text{T} - 5.9399 \times 10^{-6} \text{T}^2$
Fiber	$c = 1.8459 + 1.8306 \times 10^{-3} \text{T} - 4.6509 \times 10^{-6} \text{T}^2$
Ash	$c = 1.0926 + 1.8896 \times 10^{-3} \text{T} - 3.6817 \times 10^{-6} \text{T}^2$
Water	$c = 4.0817 - 5.3062 \times 10^{-3} T + 9.9516 \times 10^{-4} T^2$

TABLE 3 Gas compositions resulting from fuel combustion, mathematical equations for specific heat capacity, and standard chemical exergy values (van Wylen & Sonntag, 1986).

	Combustion gas			
Components	Molar fraction	Mass fraction	– Standard chemical exergy (kJ/Mol)	Specific heat capacity based on the temperature (K)
Carbon dioxide (CO ₂)	13.3	20	19.48	$0.51 + \frac{1.36T_g}{10^3} - \frac{0.796T_g^2}{10^6} + \frac{0.17T_g^3}{10^9}$
Water (H ₂ o)	12.80	8	12.39	$1.79 + \frac{0.107T_g}{10^3} + \frac{0.586T_g^2}{10^6} - \frac{0.2T_g^3}{10^9}$
Nitrogen (N ₂)	73.90	72	0.72	$1.03 - \frac{0.056T_g}{10^3} + \frac{0.288T_g^2}{10^6} - \frac{0.103T_g^3}{10^9}$
Total	100	100	-	-



Where the specific volume of the product was obtained using Equation (32) (Choi 1986):

$$v = \sum_{i} \frac{X_{i}}{\rho_{i}}.$$
 (32)

Additionally, the exergy loss associated with heat transfer from the heater wall and the pre-dryer chamber was calculated using the following equation (Soufiyan et al., 2016):

$$\dot{E}x_{I} = \left(1 - \frac{T_{0}}{T_{cw}}\right)\dot{Q}_{I.} \tag{33}$$

By formulating the exergy balance equation for each component of the dehumidifier system depicted in Figure 2, the exergy destruction rate values for these components were calculated. During exergy analysis, it is important to consider that exergy destruction rate $(\dot{E}x_D)$, arises from irreversibilities within a component, while exergy losses $(\dot{E}x_I)$, occur due to energy dissipation in the system components (Balli et al., 2007). The exergy balance equations for the dehumidifier components are as follows:

Electro-fan (EF):

$$\dot{E}x_{a1} + \dot{W} - \dot{E}x_{a2} = \dot{E}x_{D.EF} \tag{34}$$

$$(\dot{m}_{a1})ex_{a1} + \dot{W} - (\dot{m}_{a2})ex_{a2} = \dot{E}x_{D,EF}.$$
 (35)

Heater (H):

$$\dot{E}x_{a2} + \dot{E}x_{a3} + \dot{E}x_{f4} - \dot{E}x_{g5} - \dot{E}x_{a6} - \dot{E}x_{J} = \dot{E}x_{D.H}$$
 (36)

$$(\dot{m}_{a2})ex_{a2} + (\dot{m}_{a3})ex_{a3} + (\dot{m}_{f4})ex_{f4} - (\dot{m}_{g5})ex_{g5} - (\dot{m}_{a6})ex_{a6} - \dot{E}x_I = \dot{E}x_{D,H}. \tag{37}$$

Pre-dryer chamber (PC):

$$\dot{E}x_{a6} + \dot{E}x_{p7} + \dot{W} - \dot{E}x_{a8} - \dot{E}x_{p9} - \dot{E}x_{I} = \dot{E}x_{D,PC}$$
 (38)

$$(\dot{m}_{a6})ex_{a6} + (\dot{m}_{p7})ex_{p7} + \dot{W} - (\dot{m}_{a8})ex_{a8} - (\dot{m}_{p9})ex_{p9} - \dot{E}x_{l} = \dot{E}x_{D,PC}. \tag{39}$$

The exergy value plays a crucial role in quantifying the phase change of moisture within the drying chamber, and it can be determined as follows:

$$\dot{E}x_{\text{ev,dc}} = \left(1 - \frac{T_0}{T_{p,\text{dc}}}\right) \dot{Q}_{\text{ev,dc.}}$$
 (40)

2.3.3 | Evaluation of exergy efficiency and improvement potential rate

The rational exergy efficiency, process exergy efficiency, and improvement potential rate for the components of the system were determined based on the existing relationships and the schematic design of

TABLE 5 Relations of thermodynamic parameters for the components of the dehumidification system.

Component	Formulas of the output/input exergy efficiency, product/fuel exergy efficiency and improvement potential rate
Electro-fan (EF)	$\begin{split} \epsilon_{\text{EF}} &= \frac{\dot{E} \dot{x}_{\alpha 2}}{\dot{W} + \dot{E} \dot{x}_{\alpha 1}} \times 100 \\ \psi_{\text{EF}} &= \frac{\dot{E} \dot{x}_{\alpha 2} - \dot{E} \dot{x}_{\alpha 1}}{\dot{W}} \times 100 \\ \dot{I} \dot{P}_{\text{EF}} &= (1 - \varepsilon_{\text{EF}}) \left(\dot{W} + \dot{E} \dot{x}_{\alpha 1} - \dot{E} \dot{x}_{\alpha 2} \right) \end{split}$
Heater (H)	$\begin{split} \varepsilon_{H} &= \frac{\dot{E}x_{a5} + \dot{E}x_{a6}}{\dot{E}x_{a2} + \dot{E}x_{a3} + \dot{E}x_{f4}} \times 100 \\ \psi_{H} &= \frac{\dot{E}x_{a6} - \dot{E}x_{a2}}{\dot{E}x_{a3} + \dot{E}x_{f4} - \dot{E}x_{g5}} \times 100 \\ \dot{IP}_{H} &= (1 - \varepsilon_{H}) \left(\dot{E}\dot{x}_{a2} + \dot{E}\dot{x}_{a3} + \dot{E}\dot{x}_{f4} - \dot{E}\dot{x}_{g5} - \dot{E}\dot{x}_{a6} \right) \end{split}$
Pre-drying chamber (PC)	$\begin{split} \varepsilon_{PC} &= \frac{\dot{E}x_{aB} + \dot{E}x_{p9}}{\dot{E}x_{aG} + \dot{E}x_{p7} + \dot{W}} \times 100 \\ \psi_{PC} &= \frac{\dot{E}x_{eV}}{(\dot{E}x_{aG} - \dot{E}x_{aB}) + (\dot{E}x_{p7} - \dot{E}x_{p9}) + \dot{W}} \times 100 \\ I\dot{P}_{PC} &= (1 - \varepsilon_{PC}) \Big(\dot{E}x_{aG} + \dot{E}x_{p7} + \dot{W} - \dot{E}x_{aB} - \dot{E}x_{p9} \Big) \end{split}$

the dehumidifier system (Figure 1). These relationships, specific to each component, are presented individually in Table 5.

3 | RESULTS AND DISCUSSION

This section focuses on the discussion of actual thermal data obtained from the dehumidification system and the thermodynamic properties of the relevant flows. By utilizing the established relationships, the energy and exergy rates of the flows in the system were calculated, allowing for the determination of input and output exergy rates, exergy loss and destruction rates, as well as output/input and product/fuel exergy efficiencies. Additionally, the exergy improvement potential rate for each component was evaluated. Furthermore, a parametric study was conducted to analyze the impact of varying reference state temperature from 0 to 25°C on the investigated parameters of the entire dehumidification system.

3.1 | Thermodynamic evaluation of the dehumidification system

3.1.1 | Thermodynamic properties of flows and calculation of energy and exergy rates

The classification of flows within the dehumidification system and the corresponding thermodynamic values are presented in Table 6. From the table, it can be observed that the mass flow rates of air, fuel, and product in the dehumidifier (calculated using Equations (3)–(7)) are 4.29, 0.004, and 0.42 kg/s, respectively. The calculations indicate that the highest exergy rate among the input flows is associated with diesel fuel, with a value of 188.081 kW, while the lowest exergy rate is 0.093 kW for the input air flow during the combustion process.

The classification of flows within the dehumidification system and the corresponding thermodynamic values are presented in

TABLE 6 Values of energy rate, exergy rate and other thermodynamics properties related to the streams in the dehumidifier unit.

No.	Flow type	T (K)	P (kPa)	m kg/s	ω kg _{water} /kg _{air}	c kJ/kgK	Ė kW	Ėx kW
1	Intake air	300.55	101.1	4.29	0.003	1.01	118.75	5.58
2	Exhaust air	300.75	101.211	4.29	0.003	1.01	119.62	6.03
3	Inlet air	300.55	101.1	0.07	0.003	1.01	1.98	0.09
4	Fuel (diesel)	300.55	101.1	0.004		1.8	177.19	188.08
5	Combustion gases	682.98	130.3	0.07		1.16	35.99	21.06
6	Hot air	328.57	101.211	4.29	0.003	1.01	240.17	21.87
7	Input product (with 37.92% M.C.)	300.55	101.1	0.42		2.77	31.87	1.49
8	Humid air	308.01	101.1	4.31	0.009	1.02	153.66	11.15
9	Output product (with 33.84% M.C.)	308.26	101.1	0.39		2.68	37.049	2.19

TABLE 7 Exergetic inflow and outflow rates, exergetic loss rate, exergetic destruction rate, exergetic efficiencies, and improvement potential rate for the components of dehumidification system.

Component	Ėx _{in} (kW)	Ėx _{out} (kW)	Ėx _L (kW)	Ėx _D (kW)	ψ (%)	ε (%)	IP (kW)
Electro-fan	6.86	6.03	0.03	0.83	35.10	87.87	0.10
Heater	194.21	42.93	4.12	147.14	9.47	22.10	117.83
Pre-drying chamber	23.71	13.34	9.24	1.12	60.43	56.28	4.53

Table 6. From the table, it can be observed that the mass flow rates of air, fuel, and product in the dehumidifier (calculated using Equations (3)–(7)) are 4.29, 0.004, and 0.42 kg/s, respectively. The calculations indicate that the highest exergy rate among the input flows is associated with diesel fuel, with a value of 188.081 kW, while the lowest exergy rate is 0.093 kW for the input air flow during the combustion process.

3.1.2 | Exergy performance of the dehumidification system components

To assess the exergy performance of the dehumidification system, various parameters were calculated for each component. These parameters include input and output exergy rates, exergy loss rate, exergy destruction rate, output/input exergy efficiency, product/fuel exergy efficiency, and exergy improvement potential rate. By utilizing the exergy rate values obtained from Tables 3 and 6, these parameters were computed for all components in the dehumidification system, and the results are presented in Table 7. The evaluation of the dehumidification system, as depicted in Figure 2 and comprising the electro-fan, heater, and pre-dryer chamber, was based on the findings from energy and exergy analysis. The exergy parameters for these components were determined and reported in Table 7.

The results indicate that the electric power input to the electrofan and the electric motor (connected to the movable plates of the pre-dryer chamber) were 1.28 and 0.34 kW, respectively. Table 7 also reveals that the product/fuel exergy efficiency (ψ) for the electro-fan, heater, and pre-dryer chamber are 35.10%, 9.47%, and 60.43%, respectively. Furthermore, the output/input exergy efficiency for the same components was calculated as 87.87%, 22.10%, and 56.28%,

respectively. Among the system components, the electro-fan exhibited the highest exergy efficiency, while the heater had the lowest exergy efficiency. The significant exergy efficiency values for the electro-fan indicate that the output exergy rate in this component is noteworthy compared to the input exergy rate. Additionally, the heater demonstrated the highest input and output exergy rates compared to the other components. Table 7 reveals that the product/fuel exergy efficiency for the pre-dryer chamber is considerably higher than that of other components. This can be attributed to the higher mass flow rate of the product in the pre-dryer chamber, resulting from a higher evaporation rate compared to other components. In other words, as the mass of the product inside the pre-dryer chamber increases, more exergy is utilized for drying the product, leading to an increase in the exergy efficiency of the product/fuel. Another contributing factor is the lower working temperature and the higher mass flow rate of dryer air in the pre-dryer chamber compared to other components. The lower temperature facilitates a higher mass flow rate of the dryer air, which further enhances the exergy efficiency of the product/fuel in the pre-dryer chamber.

Anyway, there are effective approaches to significantly enhance the exergy efficiency of the system. One option is to utilize the humid exhaust air as a thermal medium or extract heat from the exhaust gases of the combustion process to raise the temperature of the dryer air. By incorporating a steam compressor and a secondary heat exchanger, the exergy in the output vapor from the dehumidifier can be adequately compensated, thereby strengthening the overall exergy performance. Integrating a heat exchanger unit into the dehumidification system results in reduced reliance on high-quality electrical energy and subsequently increases the exergy efficiency of the fan-heater combination (Ghasemkhani et al., 2016). Furthermore, implementing innovative techniques such as self-heat recuperation

technology, which efficiently recovers both sensible and latent heat from waste flows, can further improve the exergy performance of the dehumidification system (Matsuda et al., 2011). The recuperated exergy can be utilized to preheat intake air and natural gas for the combustion process, reducing irreversibility and enhancing system efficiency.

The pre-dryer chamber exhibits the highest exergy loss rate of 9.24 kW, primarily due to heat loss from the chamber body. On the other hand, the electro-fan experiences the lowest exergy loss rate of 0.03 kW within the same system. The exergy destruction rate in the system is most pronounced in the heater, which has an exergy destruction rate of 147.14 kW, followed by the pre-drying chamber (1.12 kW) and the electro-fan (0.83 kW). Consequently, the electrofan exhibits the lowest exergy destruction rate of 0.83 kW. The substantial exergy destruction rate in the heater is attributed to factors such as rapid mass and heat transfer, chemical reactions during combustion, and mixing processes. Several solutions, including oxygen enrichment, preheating incoming air, and reducing the air-to-fuel ratio, can mitigate these thermodynamic irreversibilities. However, implementing these solutions may lead to increased energy loss through combustion exhaust gases and heat dissipation from the components' bodies (Gümüs & Atmaca, 2013).

Improving the exergy performance of the heater in the system can be achieved by reducing irreversibilities and minimizing heat loss. It should be noted that a significant portion of exergy destruction rate in these components is inherent due to fundamental limitations. In these components, the impact of exergy destruction rate on exergy efficiency outweighs the effect of exergy loss, emphasizing that the high exergy destruction rate is the primary reason for the low exergy efficiency of components like dehumidifier heaters. However, by preventing heat transfer to the environment through insulation, it is possible to marginally enhance exergy efficiency. Implementing solutions to decrease the exergy destruction rate in the heater, such as utilizing alternative heat sources like solar energy or direct heat drying (without intermediaries), can contribute to system improvements. Additionally, it is important to note that in industrial dryers, the temperature difference between the dryer air and the product significantly influences the exergy destruction rate in the dryer chamber (Ozgener & Ozgener, 2006).

In the pre-drying chamber of the dehumidification system, the effect of exergy loss on exergy efficiency surpasses that of exergy destruction rate. This is primarily due to the significant lateral surface area of the chamber (12.29 m²), which results in a higher rate of heat loss. Therefore, by preventing exergy loss from the chamber's body, its exergy efficiency can be notably improved. The exergy efficiency of the pre-dryer chamber, which stands at 56.28%, indicates that the energy in its output can be effectively utilized for another process. Exergy recycling is feasible in two ways for components like the pre-dryer chamber: (1) Recovering exergy lost to the environment through the chamber's body, and (2) Harnessing the exergy in the moist exit air. The combined exergy from these two sources constitutes 86% and 85.06% of the input exergy for the pre-dryer chamber, respectively.

Furthermore, the overall exergy improvement potential rate for all components of the dehumidification system is calculated to be 122.46 kW, with contributions from the electro-fan, heater, and predryer chamber amounting to 0.10 kW (0.08%), 117.832 kW (96.21%), and 4.53 kW (3.70%), respectively. As a result, the heater exhibits the highest improvement potential rate among the components, followed by the pre-dryer chamber and the electro-fan in second and third positions, respectively. The significant exergy destruction rate in these components is the main factor contributing to their high improvement potential. One reason for this is the higher humidity ratio of the exit air from the pre-drying chamber (0.009) compared to that of the drying chamber (0.007). Consequently, the exergy destruction rate in the pre-dryer chamber is relatively lower than that in the dryer chamber. The improvement potential rate of each component is determined as a percentage of the total exergy input to the components. Specifically, the electro-fan, heater, and pre-dryer chamber account for 0.05%, 59.84%, and 2.30% of the total input exergy of the system, respectively.

Figure 3 illustrates the Sankey diagram showcasing the exergy flows within the dehumidifier system. As shown in Figure 3, it is evident that 75.73% (149.10 kW) of the total input exergy (196.88 kW) to the system was destroyed, while the remaining 24.27% (47.78 kW) was discharged from the system. The heater exhibited the highest exergy destruction rate, accounting for 74.74% of the total input exergy. The pre-dryer chamber and the electro-fan ranked second and third, respectively, with destruction rates of 0.57% and 0.42% of the total input exergy (Figure 3).

3.1.3 | Effect of the reference state temperature on the exergy components

To establish a standardized definition of exergy, it is essential to consider its measurement relative to the environment. In order to achieve this, a thorough characterization of the reference state conditions is required, typically involving the determination of temperature, pressure, and chemical composition. The reference state pertains to the system's equilibrium state with its surrounding environment (Al-Muslim et al., 2005; Dincer & Sahin, 2004). It is worth noting that the energy and exergy performance of operational systems are influenced by the reference state temperature and the system's operational characteristics (Ozgener & Ozgener, 2006).

The effect of the reference state temperature on the product/fuel exergy efficiency

Figure 4 illustrates the impact of increasing reference state temperature on the product/fuel exergy efficiency of the humidification system's components. The data clearly indicate that raising the reference state temperature results in a reduction in product/fuel exergy efficiency. Notably, the pre-dryer chamber exhibits the highest exergy efficiency among the system's components. Moreover, the exergy efficiency of the pre-drying chamber is most affected by the increase in reference state temperature. Specifically, when the

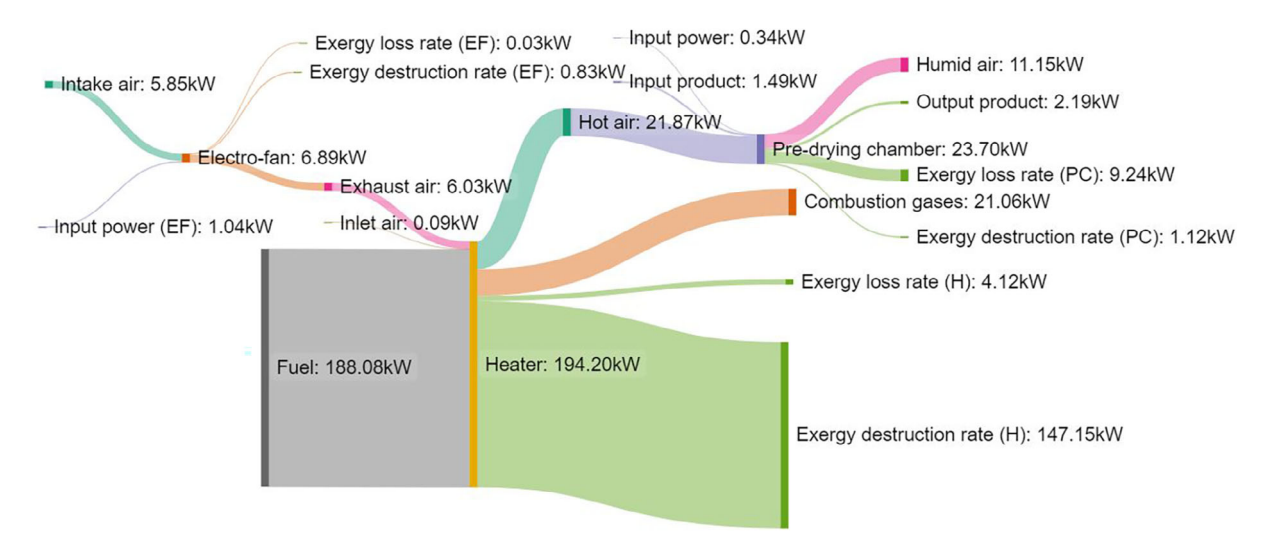


FIGURE 3 Sankey diagram of total input exergy, output exergy and the exergy destruction rate of the components of the dehumidifier system.

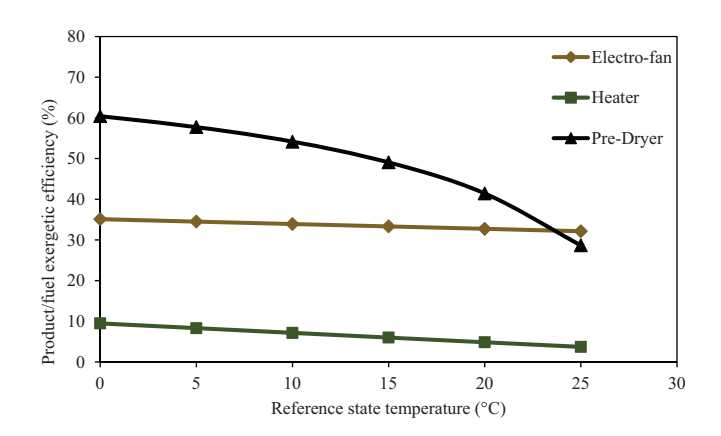


FIGURE 4 Effect of reference state temperature on the product/ fuel exergy efficiency for the components of dehumidification system.

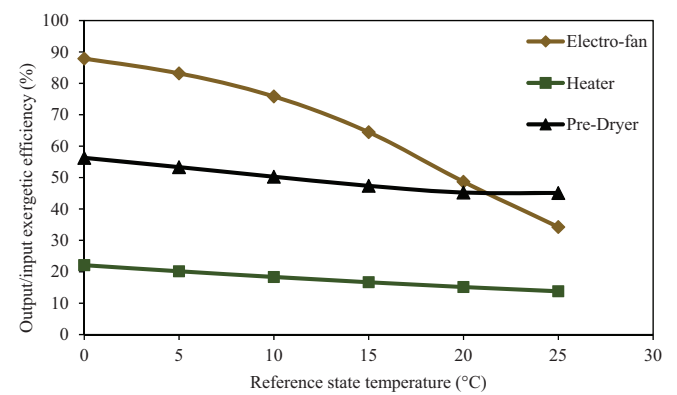


FIGURE 5 The effect of the reference state temperature on the output/input exergy efficiency of dehumidification system components.

reference state temperature rises from 0 to 25°C, the product/fuel exergy efficiency decreases from 60.43% to 28.65% (Figure 4). These findings reveal a significant decline in the product/fuel exergy efficiency for the pre-drying chamber of the humidification system at reference state temperatures exceeding 10°C. This decrease can be attributed to the higher evaporation rate associated with lower reference state temperatures. As the reference state temperature increases, the evaporation rate decreases, subsequently leading to a decrease in the product/fuel exergy efficiency for the pre-dryer chamber. Anyway, the change of the product/fuel exergy efficiency for the heater and electro-fan unlike the drying chamber with raising reference state temperature is insignificant.

The effect of reference state temperature on the output/input exergy efficiency

Figure 5 presented the effect of rising reference state temperature on the output/input exergy efficiency of the dehumidification system's

components. The figure clearly demonstrates a decline in the output/ input exergy efficiency as the reference state temperature increases. Among the components of the dehumidifier system, the electro-fan exhibits higher output/input exergy efficiency. However, the electrofan's efficiency is greatly influenced by the increase in reference state temperature. Specifically, as the reference state temperature elevates from 0 to 25°C, the electro-fan's efficiency drops from 87.87% to 34.26% (Figure 5). It is worth noting that the output/input exergy efficiency of the electro-fan component remains relatively stable until a reference state temperature of 10°C, beyond which it experiences a sharp decline while the values of the output/input exergy efficiency of the heater and pre-dryer of the dehumidification system hardly change as reference state temperature rises. In a study by Gungor et al. (2011), which focused on the drying of herbal and aromatic plants, the authors investigated the relationship between reference state temperature and exergy efficiency, concluding that there is a direct correlation between the two factors.

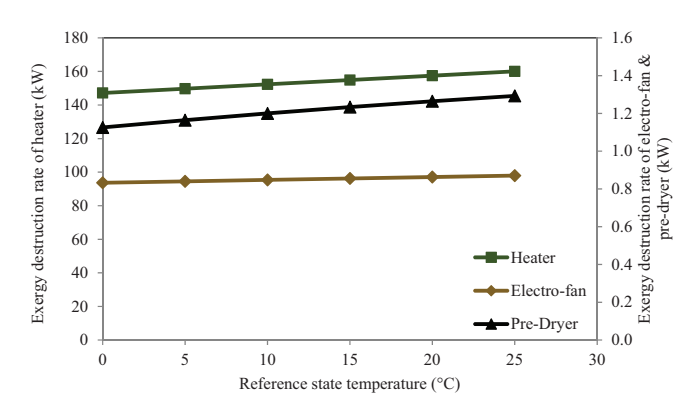


FIGURE 6 Effect of the reference state temperature on the exergy destruction rate in the components of dehumidification system.

The effect of the reference state temperature on the exergy destruction rate

The findings presented in Figure 6 illustrate the variations in the exergy destruction rate in relation to the reference state temperature for the components of the dehumidification system. Interestingly, unlike the exergy loss rate, the exergy destruction rate demonstrates an increase as the reference state temperature rises. Specifically, based on Figure 6, it is evident that the heater exhibits a significantly higher exergy destruction rate compared to the other components of the dehumidification system, as depicted in the left column of the graph. Furthermore, the reference state temperature change from 0 to 25°C has the most pronounced effect on the exergy destruction rate of the heater, resulting in an increase from 147.14 to 160.05 kW. On the other hand, the exergy destruction rate for the pre-dryer chamber and the electro-fan, displayed in the right column of the graph, experiences a much gentler slope. A noteworthy observation can be made by comparing Figures 5 and 6: there exists an inverse relationship between the exergy destruction rate and exergy efficiency.

The effect of reference state temperature on the exergy loss rate

The findings regarding the effect of reference state temperature on the exergy loss rate of the dehumidification system components in pistachio processing are presented in Figure 7. The figure clearly demonstrates that, in general, the exergy loss rate decreases as the reference state temperature increases, indicating that the majority of this exergy loss is attributed to heat dissipation from the system's components. Notably, Figure 7 highlights that the pre-dryer chamber exhibits the highest exergy loss rate within the dehumidification system. On the other hand, the exergy loss rate of the electro-fan remains nearly constant, approaching zero, and decreases from 0.038 to 0.004 kW as the reference state temperature rises from 0 to 25°C. The substantial decrease in the exergy loss rate of the pre-dryer chamber compared to the heater and electro-fan indicates that the increase in reference state temperature has the most significant effect on reducing the exergy loss rate of the pre-dryer chamber. Consequently, it can be concluded that increasing the reference state temperature effectively reduces exergy losses, particularly for the pre-dryer chamber.

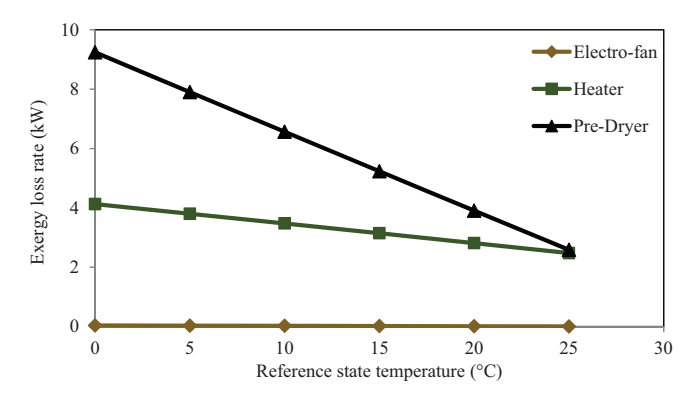


FIGURE 7 Effect of the reference state temperature on exergy loss rate in the components of dehumidification system.

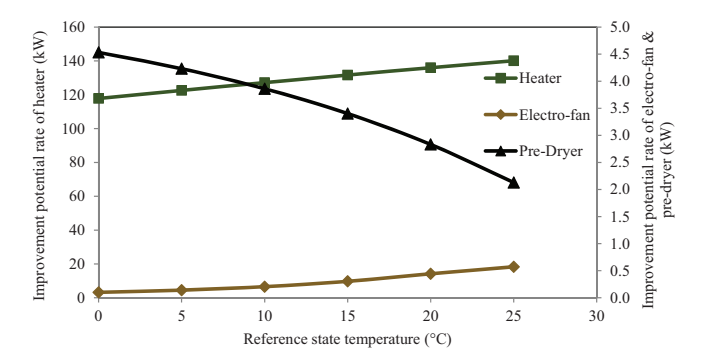


FIGURE 8 Effect of the reference state temperature on the improvement potential rate for the components of dehumidification system.

The effect of the reference state temperature on the improvement potential rate (IP)

The findings depicted in Figure 8 reveal the influence of increasing reference state temperature on the improvement potential rate of the dehumidification system's components. As shown in the Figure 8, the results indicate that, except for the pre-dryer chamber, the improvement potential rate increases as the reference state temperature rises for all components of the dehumidification system. Notably, the heater exhibits the highest improvement potential rate among the components, primarily due to its high exergy destruction rate and low exergy efficiency. Figure 8 clearly demonstrates a significant linear increase in the improvement potential rate for the heater and electro-fan as the reference state temperature increases, while a decrease is observed for the pre-dryer chamber. The impact of increasing reference state temperature on the improvement potential rate is most pronounced for the heater, where the temperature rises from 0 to 25°C leads to an increase in the improvement potential rate from 117.83 to 140.12 kW. Within the same temperature range, the improvement potential rate for the pre-dryer chamber decreases from 4.55 to 2.12 kW (Figure 8). It is important to note that the improvement potential rate values for the electro-fan and pre-dryer chamber are presented in the right column, while the values for the heater are

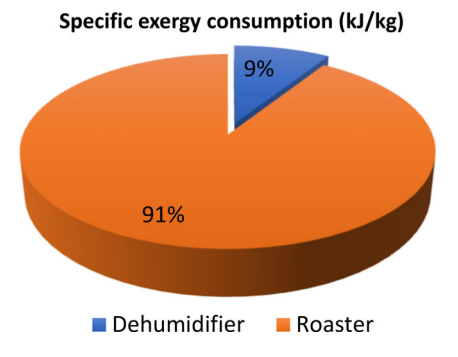


FIGURE 9 Percentile contributions of the dehumidification and roasting systems to the specific exergy consumption.



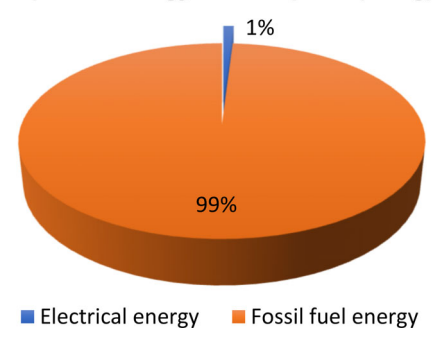


FIGURE 10 Percentile contributions of the fossil fuel energy and electrical energy to the specific exergy consumption of the processed pistachio production.

shown in the left column of Figure 8. The obtained improvement exergetic potential rate (IP) highlights the pressing need for enhancing the exergy performance of the drying operation unit.

3.1.4 | Special exergy consumption

The concept of specific exergy consumption refers to the amount of exergy utilized in drying or roasting a specific quantity of product. In the dehumidifier and roaster systems, fossil fuels and electrical energy are the sole energy sources employed. To calculate the specific exergy consumption of these systems, the exergy values of these energy sources were utilized. The specific exergy consumption values were determined as 481.85 kJ/kg for the dehumidifier system and 5027.18 kJ/kg for the roaster system. Consequently, the combined specific exergy consumption for both systems amounted to 5.50 MJ/kg. Figure 9 illustrates the respective contributions of the dehumidifier and roaster systems to the total specific exergy consumption. As depicted in Figure 9, the roaster system accounted for 91% of the total specific exergy consumption, while the dehumidifier system contributed 9% (Figure 9).

The distribution of electric energy and fossil fuels in the specific exergy consumption of the two systems is illustrated in Figure 10.

The figure reveals that fossil fuels (diesel and natural gas) contribute to 99% of the total specific exergy consumption, while electrical energy accounts for only 1%. Hence, significant reductions in the specific exergy consumption of these systems can be achieved by optimizing the dehumidifier heater, roasting furnace, and drying heater, along with implementing suitable solutions.

After a thorough examination and thermodynamic evaluation of the humidification system in the processed pistachio production unit using energy and exergy analysis, and implementing suitable measures to mitigate exergy loss and destruction rate, the findings indicate that this approach offers a viable solution for process optimization and enhancing the performance of the final production system for processed pistachios. These results hold potential for future research and practical applications in the field.

4 | CONCLUSION

In the current study, the exergy performance of a dehumidifier system integrated with a common industrial dryer for raw pistachio processing was examined. Actual thermal data and mass, energy, and exergy balances were used to evaluate the energy and exergy parameters of the unit. The effect of reference state temperature on the exergy parameters was also investigated. The findings revealed that the overall exergy efficiency of the dehumidifier was 17.47%. The electro-fan exhibited the highest exergy efficiency, while the heater had the lowest. The heater was identified as the component with the highest exergy destruction rate, whereas the electro-fan had the lowest. The pre-dryer chamber showed the highest exergy loss rate, whereas the electro-fan had the lowest. Furthermore, an increase in reference state temperature led to a decrease in exergy loss rate, an increase in exergy destruction rate, a decrease in exergy efficiency, and an increase in the improvement potential rate for the dehumidifier system components. The specific exergy consumption for the dehumidifier system was measured at 481.58 kJ/kg, indicating its high specific exergy consumption. Overall, conducting exergy analysis for such systems can offer a comprehensive and practical approach to reducing capital costs in pistachio production lines, achieving energy savings, and enhancing the performance of industrial system components for engineers and factory owners. It is worth noting that exergy analysis, accounting for irreversibility aspects, plays a crucial role in estimating optimal performance conditions for the investigated system.

NOMENCLATURES

Notations

m mass flow rate (kg/s)

T temperature (°C or K)

P atmospheric pressure (kPa)

h enthalpy (kJ/kg)

 h_{fg} latent heat of vaporization (kJ/kg)

 c_p specific heat (kJ/kg°C)

R	gas constant ((8.3143	kJ/	mol)
---	----------------	---------	-----	------

- R universal gas constant (8.314 J mol/K)
- En energy rate (kW)
- Q heat transfer rate (kW)
- www work rate (kW/s)
- Ex exergy rate (kW)
- ex specific exergy (kJ/kg)
- IP improvement potential rate (kW)
- LHV lower heat value (kJ/kg)
- V voltage (V)
 I current (A)
- y mass fraction (–)
- X mole fraction (–)
- n specific mole number (mol/kg)
- a carbon number of hydrocarbon fuels
- b hydrogen number of hydrocarbon fuels

Greek letters

- v specific volume (kg/m³)
- n efficiency (%)
- γ fuel quality factor (–)
- ε output/input exergy efficiency (%)
- ψ fuel/product exergy efficiency (%)
- φ relative humidity of air (%)
- ω humidity ratio (kg water/ kg dry air)
- δ standard chemical exergy (kJ/mol)
- ρ density (kg/m³)

Subscripts

- 0 reference state
- a air
- cw chamber wall
- vs saturated vapor
- 0 initial
- in inlet air
- out output
- a air
- p product
- g gas
- v constant volume
- f fuel
- w water
- i each component
- cg combustion gas
- I loss
- D destruction
- ex exergy
- ph physical
- ch chemical
- pt potential kn kinetic
- mech mechanical
- elec electrical

- each component
- P pressure
- fg fuel-gas
- ev evaporator

ACKNOWLEDGMENTS

The authors would like to extend their appreciations for financial support provided by the University of Jiroft.

CONFLICT OF INTEREST STATEMENT

The authors declare no conflict of interest.

DATA AVAILABILITY STATEMENT

The data that support the findings of this study are available from the corresponding author upon reasonable request.

ORCID

Majid Dowlati https://orcid.org/0000-0001-7312-5291

REFERENCES

- Afzal, T. M., Abe, T., & Hikida, Y. (1999). Energy and quality aspects during combined FIR-convection drying of barley. *Journal of Food Engineering*, 42(4), 177–182. https://doi.org/10.1016/S0260-8774(99) 00117-X
- Akpinar, E. K. (2004). Energy and exergy analyses of drying of red pepper slices in a convective type dryer. *International Communications in Heat and Mass Transfer*, 31(8), 1165–1176. https://doi.org/10.1016/j.icheatmasstransfer.2004.08.014
- Al-Muslim, H., Dincer, I., & Zubair, S. M. (2005). Effect of reference state on exergy efficiencies of one-and two-stage crude oil distillation plants. *International Journal of Thermal Sciences*, 44(1), 65–73. https://doi.org/10.1016/j.ijthermalsci.2004.04.015
- Amiri Chayjan, R., Kaveh, M., Dibagar, N., & Zarrin Nejad, M. (2017). Optimization of pistachio nut drying in a fluidized bed dryer with microwave pretreatment applying response surface methodology. *Chemical Product and Process Modeling*, 12(3), 20160048. https://doi.org/10.1515/cppm-2016-0048
- Argo, B. D., & Ubaidillah, U. (2020). Thin-layer drying of cassava chips in multipurpose convective tray dryer: Energy and exergy analyses. *Journal of Mechanical Science and Technology*, 34, 435–442. https://doi.org/10.1007/s12206-019-1242-9
- ASAE-American Society of Agricultural Engineers. (2005. Available from: http://engineering.purdue.edu/~abe305/moisture/html/page14.htm). Standard for measurement of moisture in grin and seed. Agricultural Engineers Yearbook. Access on: Aug. 10, 2010.
- Balli, O., Aras, H., & Hepbasli, A. (2007). Exergetic performance evaluation of a combined heat and power (CHP) system in Turkey. *International Journal of Energy Research*, 31(9), 849–866. https://doi.org/10.1002/er.1270
- Bapat, S. M., Majali, V. S., & Ravindranath, G. (2016). Exergy and sustainability analysis of quintuple effect evaporation unit in a sugar industry-a case study. *International Journal of Renewable Energy Technology*, 7(1), 46–68. https://doi.org/10.1504/JJRET.2016.073401
- Beigi, M. (2022). Dehydration behavior and thermodynamic analysis of kiwifruit slices in convective tray dryer: Kiwifruit drying. Latin American Applied Research-an International Journal, 52(2), 119–126. https:// doi.org/10.52292/j.laar.2022.813
- Bejan, A. (1988). Advanced engineering thermodynamics. John Wiley & Sons.

- Chemmala, F., & Dinesh, L. R. (2014). Exergy analysis of solar energy applications and renewable energy systems. In Int. conf. On advanced trends in engineering and technology (pp. 254–257). Forschung Publications.
- Choi, Y. (1986). Effects of temperature and composition on the thermal properties of foods. Food Engineering and Process Applications, 1, 93–101
- Colak, N., Erbay, Z., & Hepbasli, A. (2013). Performance assessment and optimization of industrial pasta drying. *International Journal of Energy Research*, 37(8), 913–922. https://doi.org/10.1002/er.2895
- Corzo, O., Bracho, N., Vásquez, A., & Pereira, A. (2008). Energy and exergy analyses of thin layer drying of coroba slices. *Journal of Food Engineer*ing, 86(2), 151–161. https://doi.org/10.1016/j.jfoodeng.2007.05.008
- Coskun, C., Bayraktar, M., Oktay, Z., & Dincer, I. (2009). Energy and exergy analyses of an industrial wood chips drying process. *International Jour*nal of Low-Carbon Technologies, 4(4), 224–229. https://doi.org/10. 1093/iilct/ctp024
- Dincer, I., & Cengel, Y. A. (2001). Energy, entropy and exergy concepts and their roles in thermal engineering. *Entropy*, 3(3), 116–149. https://doi. org/10.3390/e3030116
- Dincer, I., & Sahin, A. Z. (2004). A new model for thermodynamic analysis of a drying process. *International Journal of Heat and Mass Transfer*, 47(4), 645–652. https://doi.org/10.1016/j.ijheatmasstransfer.2003. 08.013
- Dowlati, M., Aghbashlo, M., & Soufiyan, M. M. (2017). Exergetic performance analysis of an ice-cream manufacturing plant: A comprehensive survey. Energy, 123, 445–459. https://doi.org/10.1016/j.energy.2017.02.007
- FAO. (2021). FAO Stat Database. Retrieved from http://faostat.fao.org
- Gamlı, Ö. F., & Hayoğlu, İ. (2007). The effect of the different packaging and storage conditions on the quality of pistachio nut paste. *Journal of Food Engineering*, 78(2), 443–448. https://doi.org/10.1016/j.jfoodeng. 2005.10.013
- Ghasemkhani, H., Keyhani, A., Aghbashlo, M., Rafiee, S., & Mujumdar, A. S. (2016). Improving exergetic performance parameters of a rotating-tray air dryer via a simple heat exchanger. *Applied Thermal Engineering*, 94, 13–23. https://doi.org/10.1016/j.applthermaleng.2015.10.114
- Golpour, I., Kaveh, M., Chayjan, R. A., & Guiné, R. P. (2020). Energetic and exergetic analysis of a convective drier: A case study of potato drying process. *Open Agriculture*, 5(1), 563–572. https://doi.org/10.1515/ opag-2020-0058
- Gümüş, M., & Atmaca, M. (2013). Energy and exergy analyses applied to a CI engine fueled with diesel and natural gas. Energy Sources, Part A: Recovery, Utilization, and Environmental Effects, 35(11), 1017–1027. https://doi.org/10.1080/15567036.2010.516312
- Gungor, A., Erbay, Z., & Hepbasli, A. (2011). Exergoeconomic analyses of a gas engine driven heat pump drier and food drying process. *Applied Energy*, 88(8), 2677–2684. https://doi.org/10.1016/j.apenergy.2011. 02.001
- Heldman, D. R., & Singh, R. P. (1981). Food process engineering (2nd ed., p. 273). Avi Publishing Co., Inc.
- Hepbasli, A., Erbay, Z., Çolak, N., Hancioglu, E., & İçier, F. (2010). An exergetic performance assessment of three different food driers. Proceedings of the Institution of Mechanical Engineers, Part A: Journal of Power and Energy, 224(1), 1–12. https://doi.org/10.1243/09576509JPE802
- Hogerwaard, J. (2014). Comparative study of ammonia-based clean rail transportation systems for greater Toronto area. (*Doctoral dissertation*).
- Hsu, M. H., Mannapperuma, J. D., & Singh, R. P. (1991). Physical and thermal properties of pistachios. *Journal of Agricultural Engineering Research*, 49, 311–321. https://doi.org/10.1016/0021-8634(91) 80047-I
- Kader, A. A., Heintz, C. M., Labavitch, J. M., & Rae, H. L. (1982). Studies related to the description and evaluation of pistachio nut quality1. *Journal of the American Society for Horticultural Science*, 107(5), 812–816. https://doi.org/10.21273/JASHS.107.5.812

- Karami, H., Kaveh, M., Golpour, I., Khalife, E., Rusinek, R., Dobrzański, B., Jr., & Gancarz, M. (2021). Thermodynamic evaluation of the forced convective hybrid-solar dryer during drying process of rosemary (Rosmarinus officinalis L.) leaves. *Energies*, 14(18), 5835. https://doi. org/10.3390/en14185835
- Kashani Nejad, M., Tabil, L. G., Mortazavi, A., & Safe Kordi, A. (2003). Effect of drying methods on quality of pistachio nuts. *Drying Technology*, 21(5), 821–838. https://doi.org/10.1081/DRT-120021688
- Kaveh, M., Abbaspour-Gilandeh, Y., & Chen, G. (2020). Drying kinetic, quality, energy and exergy performance of hot air-rotary drum drying of green peas using adaptive neuro-fuzzy inference system. Food and Bioproducts Processing, 124, 168–183. https://doi.org/10.1016/j.fbp. 2020.08.011
- Kaveh, M., Chayjan, R. A., Golpour, I., Poncet, S., Seirafi, F., & Khezri, B. (2021). Evaluation of exergy performance and onion drying properties in a multi-stage semi-industrial continuous dryer: Artificial neural networks (ANNs) and ANFIS models. Food and Bioproducts Processing, 127, 58–76. https://doi.org/10.1016/j.fbp.2021.02.010
- Khan, N. B. N., Barifcani, A., Tade, M., & Pareek, V. (2016). A case study: Application of energy and exergy analysis for enhancing the process efficiency of a three stage propane pre-cooling cycle of the cascade LNG process. *Journal of Natural Gas Science and Engineering*, 29, 125– 133. https://doi.org/10.1016/j.jngse.2015.12.034
- Kim, K. M., Yun, N., Jeon, Y. H., Lee, D. H., Cho, H. H., & Kang, S. H. (2010). Conjugated heat transfer and temperature distributions in a gas turbine combustion liner under base-load operation. *Journal of Mechanical Science and Technology*, 24, 1939–1946. https://doi.org/ 10.1007/s12206-010-0625-8
- Kotas, T. J. (1995). The exergy method of thermal plant analysis. Krieger.
- Kouchakzadeh, A., & Haghighi, K. (2011). Modeling of vacuum-infrared drying of pistachios. Agricultural Engineering International: CIGR Journal, 13(3), 1–7.
- Kumar, M., Sahdev, R. K., Tawfik, M. A., & Elboughdiri, N. (2023). Natural convective greenhouse vermicelli drying: Thermo-environ-econokinetic analyses. Sustainable Energy Technologies and Assessments, 55, 103002. https://doi.org/10.1016/j.seta.2022.103002
- Mandalari, G., Barreca, D., Gervasi, T., Roussell, M. A., Klein, B., Feeney, M. J., & Carughi, A. (2021). Pistachio nuts (Pistacia vera L.): Production, nutrients, bioactives and novel health effects. *Plants*, 11(1), 18. https://doi.org/10.3390/plants11010018
- Matsuda, K., Kawazuishi, K., Kansha, Y., Fushimi, C., Nagao, M., Kunikiyo, H., & Tsutsumi, A. (2011). Advanced energy saving in distillation process with self-heat recuperation technology. *Energy*, 36(8), 4640–4645. https://doi.org/10.1016/j.energy.2011.03.042
- Mokhtarian, M., Tavakolipour, H., & Kalbasi-Ashtari, A. (2016). Energy and exergy analysis in solar drying of pistachio with air recycling system. Drying Technology, 34(12), 1484–1500. https://doi.org/10.1080/07373937.2015.1129499
- Moran, M. J., Shapiro, H. N., Boettner, D. D., & Bailey, M. B. (2010). Fundamentals of engineering thermodynamics. John Wiley & Sons.
- Noguera-Artiaga, L., Sánchez-Bravo, P., Pérez-López, D., Szumny, A., Calin-Sánchez, Á., Burgos-Hernández, A., & Carbonell-Barrachina, Á. A. (2020). Volatile, sensory and functional properties of hydrosos pistachios. Food, 9(2), 158. https://doi.org/10.3390/foods9020158
- Nwosu-Obieogu, K., Oke, E. O., & Bright, S. (2022). Energy and exergy analysis of three leaved yam starch drying in a tray dryer: Parametric, modelling and optimization studies. *Heliyon*, *8*(8), e10124. https://doi.org/10.1016/j.heliyon.2022.e10124
- Okunola, A. A., Adekanye, T. A., Okonkwo, C. E., Kaveh, M., Szymanek, M., Idahosa, E. O., Olayanju, A. T., & Wojciechowska, K. (2023). Drying characteristics, kinetic modeling, energy and exergy analyses of water yam (Dioscorea alata) in a hot air dryer. *Energies*, 16(4), 1569. https://doi.org/10.3390/en16041569
- Omid, M., Baharlooei, A., & Ahmadi, H. (2009). Modeling drying kinetics of pistachio nuts with multilayer feed-forward neural network. *Drying*

- Technology, 27(10), 1069-1077. https://doi.org/10.1080/07373930903218602
- Özahi, E., & Demir, H. (2013). A model for the thermodynamic analysis in a batch type fluidized bed dryer. *Energy*, *59*, 617–624. https://doi.org/10.1016/j.energy.2013.07.001
- Ozgener, L., & Ozgener, O. (2006). Exergy analysis of industrial pasta drying process. *International Journal of Energy Research*, 30(15), 1323–1335. https://doi.org/10.1002/er.1227
- Parhizi, Z., Karami, H., Golpour, I., Kaveh, M., Szymanek, M., Blanco-Marigorta, A. M., Marcos, J. D., Khalife, E., Skowron, S., Adnan Othman, N., & Darvishi, Y. (2022). Modeling and optimization of energy and exergy parameters of a hybrid-solar dryer for basil leaf drying using RSM. Sustainability, 14(14), 8839. https://doi.org/10.3390/su14148839
- Rodriguez, L. (1980). Calculation of available-energy quantities. https://doi.org/10.1021/bk-1980-0122.ch003
- Shen, F., Wang, M., Huang, L., & Qian, F. (2021). Exergy analysis and multiobjective optimisation for energy system: A case study of a separation process in ethylene manufacturing. *Journal of Industrial and Engineering Chemistry*, 93, 394–406. https://doi.org/10.1016/j.jiec.2020.10.018
- Soufiyan, M. M., & Aghbashlo, M. (2017). Application of exergy analysis to the dairy industry: A case study of yogurt drink production plant. Food and Bioproducts Processing, 101, 118–131. https://doi.org/10.1016/j. fbp.2016.10.008
- Soufiyan, M. M., Dadak, A., Hosseini, S. S., Nasiri, F., Dowlati, M., Tahmasebi, M., & Aghbashlo, M. (2016). Comprehensive exergy analysis of a commercial tomato paste plant with a double-effect evaporator. *Energy*, 111, 910–922. https://doi.org/10.1016/j.energy.2016. 06.030
- Strumiłło, C., Jones, P. L., & Zylla, R. (1995). Energy aspects in drying. *Handbook of industrial drying*, 2, 1241–1275.
- Tinoco-Caicedo, D. L., Lozano-Medina, A., & Blanco-Marigorta, A. M. (2020). Conventional and advanced exergy and exergoeconomic analysis of a spray drying system: A case study of an instant coffee factory in Ecuador. *Energies*, 13(21), 5622. https://doi.org/10.3390/en13215622
- van Wylen, G. J., & Sonntag, R. E. (1986). Fundamentals of classical thermodynamics; English/SI version. John Wiley & Sons.

- Vilarinho, A. N., Campos, J. B., & Pinho, C. (2017). Energy and exergy analysis of a pre-distillation unit. *International Journal of Thermodynamics*, 20(2), 91–100. https://doi.org/10.2298/TSCI210522311J
- Yan, J., Wei, H., Wu, H., You, Z., & Xie, H. (2023). Thermodynamics and non-uniformity in convective reversing drying wheat. *Applied Thermal Engineering*, 231, 120948. https://doi.org/10.1016/j.applthermaleng.2023.120948
- Zadhossein, S., Abbaspour-Gilandeh, Y., Kaveh, M., Nadimi, M., & Paliwal, J. (2023). Comparison of the energy and exergy parameters in cantaloupe (*Cucurbita maxima*) drying using hot air. *Smart Agricultural Technology*, 4, 100198. https://doi.org/10.1016/j.atech.2023.100198
- Zalazar-Garcia, D., Román, M. C., Fernandez, A., Asensio, D., Zhang, X., Fabani, M. P., Rodriguez, R., & Mazza, G. (2022). Exergy, energy, and sustainability assessments applied to RSM optimization of integrated convective air-drying with pretreatments to improve the nutritional quality of pumpkin seeds. Sustainable Energy Technologies and Assessments, 49, 101763. https://doi.org/10.1016/j.seta.2021.101763
- Zeng, Z., Li, B., Han, C., Wu, W., Chen, T., Dong, C., & Zhang, F. (2022). Performance of exergetic, energetic and techno-economic analyses on a gas-type industrial drying system of black tea. *Food*, 11(20), 3281. https://doi.org/10.3390/foods11203281
- Zohrabi, S., Aghbashlo, M., Seiiedlou, S. S., Scaar, H., & Mellmann, J. (2020). Energy saving in a convective dryer by using novel real-time exergy-based control schemes adjusting exhaust air recirculation. *Journal of Cleaner Production*, 257, 120394. https://doi.org/10.1016/j.jclepro.2020.120394

How to cite this article: Dowlati, M., Golpour, I., Blanco-Marigorta, A. M., Marcos, J. D., de la Guardia, M., & Sheikhshoaei, H. (2023). A comprehensive assessment of energetic and exergetic performance for the dehumidification system of a processed pistachio production unit. *Journal of Food Process Engineering*, e14471. https://doi.org/10.1111/jfpe.14471